



**HAL**  
open science

## Syngas biomethanation: Study of process performances at high syngas flow rate in pressurized stirred column

J. Figueras, H. Benbelkacem, C. Dumas, P. Buffiere

### ► To cite this version:

J. Figueras, H. Benbelkacem, C. Dumas, P. Buffiere. Syngas biomethanation: Study of process performances at high syngas flow rate in pressurized stirred column. *Bioresource Technology*, 2023, 376, pp.128936. 10.1016/j.biortech.2023.128936 . hal-04260457

**HAL Id: hal-04260457**

**<https://hal.science/hal-04260457>**

Submitted on 26 Oct 2023

**HAL** is a multi-disciplinary open access archive for the deposit and dissemination of scientific research documents, whether they are published or not. The documents may come from teaching and research institutions in France or abroad, or from public or private research centers.

L'archive ouverte pluridisciplinaire **HAL**, est destinée au dépôt et à la diffusion de documents scientifiques de niveau recherche, publiés ou non, émanant des établissements d'enseignement et de recherche français ou étrangers, des laboratoires publics ou privés.

# Syngas biomethanation: study of process performances at high syngas flow rate in pressurized stirred column

J. Figueras<sup>a,b\*</sup>, H. Benbelkacem<sup>a</sup>, C. Dumas<sup>c</sup>, and P. Buffiere<sup>a</sup>

<sup>a</sup>*Univ Lyon, INSA Lyon, DEEP, EA7429, 69621 Villeurbanne, France*

<sup>b</sup>*ENOSIS, 31100 Toulouse, France*

<sup>c</sup>*TBI, University of Toulouse, INSA, INRAE, CNRS, Toulouse, France*

*\*Corresponding author: Julie Figueras; Tel.: +336 16 81 75 13; E-mail: julie.figueras@insa-lyon.fr*

## Abstract

Syngas biomethanation is a promising technology for waste to energy conversion. However, it had not yet been tested at high syngas flow rates. The aim of this study was to assess the possibility for syngas biomethanation to reach high methane productivity at higher syngas inflow rate. A pressurized stirred column was implemented. The syngas inflow rate was gradually increased, and two different increase strategies were compared. The highest methane productivity achieved yet with syngas-biomethanation was obtained, with 23.2 L<sub>CH<sub>4</sub></sub>/L/d, with high conversion efficiencies of 89% for H<sub>2</sub> and 82% for CO. The mass transfer performances of the process were investigated, and the existence of a biological enhancement factor was observed. Considering an enhancement factor in bioprocesses is a pioneering concept that could change the way we design bioreactor to improve mass transfer. The high methane productivity obtained in this study paves the way for the process industrialization.

**Keywords** : Biological methanation ; synthesis gas ; fermentation ; carbon monoxide conversion ; biological enhancement factor

# 1 Introduction

The increasing waste production induces stress on the environment, such as greenhouse gas emissions, increasing landfill space usage and water and soil pollution (Dolk et al., 1998; Palmiotto et al., 2014). An interesting waste management approach is the waste to energy strategy. It presents many advantages, including waste volume and mass reduction and reduced greenhouse gas emissions (Arena, 2012). Moreover, waste-based energy production can be considered part of the greater strategy to phase out fossil fuel use (Vehlow et al., 2007). In this sense, pyro-gasification is a promising approach to convert waste to energy (Tanigaki et al., 2015). Indeed, this process could allow for hard to process waste, such as lignocellulosic biomass or heterogenous municipal solid to be upgraded to energy.

The pyro-gasification of waste produces multiple components such as bio-oil, bio char and synthetic gas (syngas) (Tsui and Wong, 2019). Syngas is a mixture of hydrogen, carbon monoxide, carbon dioxide and methane. To improve the calorific value of syngas, it can be upgraded to methane. Another advantage of this transformation is the use of the already existing natural gas grid and storage infrastructures.

To convert syngas to methane, biological methanation is an interesting innovation. The methanation reactions are operated by microorganisms that act as catalyst while supporting their growth. The mild operating conditions (temperature inferior to 70°C and low pressure) allow low energy consumption compared to catalytic methanation (Grimalt-Alemany et al., 2018). Moreover, the microorganisms can be adapted from anaerobic sewage or manure sludge which is also cost effective.

When using a mixed microbial consortium, biomethanation is operated through complex interactions and syntrophic associations. Temperature conditions play an important part on the

main biological routes and methane productivity. Indeed, thermophilic conditions appear to allow higher methane productivity than mesophilic conditions (Asimakopoulos et al., 2020; Grimalt-Alemany et al., 2019; Youngsukkasem et al., 2015). Therefore, thermophilic conditions are more suitable for an intensified process. In thermophilic conditions, studies have shown that two reactions are predominant (Grimalt-Alemany et al., 2019; Figueras et al., 2021; Guiot et al., 2011; Sipma et al., 2003). One is CO conversion to H<sub>2</sub> and CO<sub>2</sub> through biological water-gas shift (Eq. 1) by carboxydophilic hydrogenogens and the other H<sub>2</sub> and CO<sub>2</sub> conversion to methane by hydrogenotrophic methanogens (Eq. 2).



When considering biomethanation performances, one should consider the gas-liquid mass transfer capability of the system. Indeed, the gaseous substrate (syngas) must be transferred to the microorganisms that are in the liquid phase. Generally, this is the limiting step regarding the rates of the process (Asimakopoulos et al., 2018). The maximum gas-liquid mass transfer rate of a component *i* is expressed by Eq. 3:

$$N_{\max,i} = k_{L,i} * H_{i, cp} * P_i \quad (3)$$

With  $P_i$  the partial pressure (bar) of the component *i*,  $H_{i, cp}$  the Henry law constant (mol/L/bar) and  $k_{L,i}$  the mass transfer coefficient of *i* (1/d). Therefore, to improve the mass transfer rate, one can improve the  $k_{L,i}$  with an optimized reactor configuration, with systems such as packing bed, hollow membrane reactors or stirred tank reactor (Jensen et al., 2021). Moreover, according to Eq. 3, the maximum mass transfer rate can be improved by enhancing the partial pressure of the reactor. It is

the strategy presented in this study, with a tank pressurized at 4 bar. Furthermore, in this study the  $k_{La}$  is improved with continuous agitation.

Although syngas-biomethanation is a promising technology, it has not been tested at large scale yet. To our knowledge, prior to this study, the highest syngas inflow rate tested was 65.8  $L_{STP}/L_{bed}/d$  (STP: standard temperature and pressure) by Asimakopoulos et al. (2021b). They obtained the highest methane productivity achieved yet of 9.5  $L_{STP}/L_{bed}/d$ , with conversion efficiencies of 76% for CO ( $E_{CO}$ ) and 97% for H<sub>2</sub> ( $E_{H_2}$ ) in thermophilic conditions. Higher syngas inflow rates should be tested to assess the limits of the biological consortium and to prove that the syngas-biomethanation is compatible for industrialization. It is therefore the aim of this study.

The consortium used in this study had been previously adapted for syngas-biomethanation. The aim was to determine CO and H<sub>2</sub> conversion rates and CH<sub>4</sub> productivities for various syngas inflow rates. Another objective was to determine whereas the system was sensitive to rapid changes in input feed rate. Thus, a continuous lab-scale pressurized tank was implemented with syngas inflow rate ranging from 18.0  $L_{STP}/L/d$  to 135.6  $L_{STP}/L/d$ . Two different strategies for the inflow increase were studied and compared. Methane productivities were compared to the scientific literature.

## 2 Materials and Methods

### 2.1 Inoculation and Operating Conditions

The reactor set-up and the analytical methods used in this work are detailed in a previous article (Figueras et al., 2021). The reactor was a 12L stainless steel gastight stirred tank with continuous gas injection (Fig. 1). The working volume was 10L. The injected syngas was obtained from gas bottles for CO and CO<sub>2</sub> and from a hydrogen generator for H<sub>2</sub>. The syngas composition and inflow rate were adjusted with three mass flow controllers, one for each gas. The syngas composition was

set to 40% CO, 40% H<sub>2</sub> and 20% CO<sub>2</sub>. According to the stoichiometry of the reactions involved in syngas biomethanation (Eq. 1 and 2), considering full conversion, such a syngas composition should not produce nor consumed water. This indicates that the liquid medium should not be diluted as biomethanation takes place.

The pressure was regulated at  $4.000 \pm 0.001$  bars with a pressure controller. The outlet gas flow rate was measured with a volumetric flow rate counter and its composition with micro gas chromatography. The tank was thermoregulated at  $55 \pm 1$  °C with a temperature-controlled thermostat circulating hot water in the water jacket of the tank. The reactor was agitated at 1000 rpm thanks to an electric motor and three Rushton turbines. A solution of Na<sub>2</sub>S was injected daily in the pressurized tank with a dosing pump. pH was stable between 6.3 and 6.7 without any regulation.

The reactor was initially inoculated with a mesophilic sludge from the wastewater treatment plant of La Feyssine, Lyon, France. It was then specialized by being exposed to the operating conditions of syngas biomethanation at high pressure (4 bar). The reactor reached stable methane production after a few months of adaptation, which is detailed in a previous study (Figueras et al., 2021). The adapted consortium was then operated during approximately 10 months.

To study the performances of the process, the syngas inflow rate was gradually increased by 20% steps, from 18.0 L<sub>STP</sub>/L/d to 135.6 L<sub>STP</sub>/L/d, at 4 bar. At each step of tested syngas inflow rate, the inflow rate was maintained for a certain time. To ensure sufficient biomass growth, each step of tested syngas inflow rate was first maintained for approximately 24h (experiment A). The step duration was then reduced to approximately 3h to see if the process could be sped up and if high methane productivities could be reached quicker (experiment B). The flow rates were not increased during the weekends, leading to longer step durations. For each experiment, the process

performance at atmospheric pressure at low inflow rate of 18.0 L<sub>STP</sub>/L/d were also studied.

Experiment A and B were separated from each other by a 4 months period during which the biomethanation reactor was not interrupted. The two experiments are displayed in Fig. 2.

Experiment A started with an initial total solid (TS) concentration of  $8.5 \pm 0.1$  g/L and an initial volatile solid (VS) concentration of  $5.4 \pm 0.1$  g/L. To guarantee no ammonium deficiency, the initial concentration of  $\text{NH}_4^+$  was set at  $1407 \pm 8$  mg/L with an initial addition of  $\text{NH}_4\text{OH}$  (25%).

Regarding experiment B, the initial TS concentration was  $11.5 \pm 0.1$  g/L, and the initial VS concentration was  $6.8 \pm 0.1$  g/L. The difference between the initial concentrations between experiment A and B can be explained by the fact that the reactor produced methane during 4 months between the experiments, leading to an increase in biomass concentrations. The initial  $\text{NH}_4^+$  concentration was set at  $1320 \pm 3$  mg/L for experiment B.

In experiment A, 10 mL of a solution of  $\text{Na}_2\text{S}$  (16.2 g/L) was supplied daily to the reactor using a dosing pump. In experiment B, the supply was increased due apparent sulphur deficiencies observed between the two experiments. The supply was increased accordingly to methane production to limit sulphur deficiencies and a total of 84 mL was injected over the course of experiment B.

The mean pH was  $6.6 \pm 0.1$  and  $6.3 \pm 0.1$  during experiment A and B, respectively.

In experiment A, the reactor was depressurized every 3 to 4 days to sample 200 mL of inoculum to perform liquid analysis. To maintain a constant liquid volume in the tank, the liquid level was adjusted after sampling with a solution of nutrients (0.143 mg/L B, 0.008 mg/L Co, 0.186 mg/L Cu, 0.192 mg/L Fe, 127 mg/L K, 22.6 mg/L Mg, 0.041 mg/L Ni, 5.09 mg/L S, 0.176 mg/L Zn, 714 mg/L

NH<sub>4</sub><sup>+</sup>). In experiment B, since the experiment lasted about 4 days, the medium was analysed only at the beginning and at the end of the experiment.

Liquid analysis on the medium included Volatile Fatty Acid (VFA), ammonium, trace elements, TS and VS, and water-soluble chemical oxygen demand (COD). All analyses excepting TS and VS were performed after centrifugation and filtration at 0.45 µm. All the analytical methods are detailed in a previous article (Figueras et al., 2021).

## 2.2 Mass transfer characterization

The mass transfer coefficient  $k_{La}$  was characterized with O<sub>2</sub> reoxygenation method in clean water (10 L) according to He et al. (2003). The dissolved oxygen concentration was measured using an EasySense O<sub>2</sub> 21 probe (Mettler Toledo, Switzerland). The reactor was first deoxygenated with nitrogen, then reoxygenated with air. The reoxygenated curve was then used to determine the  $k_{La}$ . Different actual inflow rates of air were tested, from  $26 \pm 14$  L/d to  $1613 \pm 17$  L/d at 55°C.

The impact of pressure was studied from 1.00 to 1.75 bar only, due to the low-pressure tolerance of the oxygen probe. To consider the impact of pressure on the  $k_{La}$ , the inflow rate was converted into the actual inflow rate injected in the tank. It was therefore corrected for temperature and pressure. For instance, a syngas inflow rate of 18.0 L<sub>STP</sub>/L/d (0°C, 1 bar) corresponds to an actual flow rate of 5.4 L/L/d at 55°C and 4 bar.

It was observed that the pressure mostly had an impact on the  $k_{La}$  due to volumetric reduction of the gas (Jensen et al., 2021). Therefore, the  $k_{La}$  was correlated with the actual flow rate to consider the impact of the pressure. More data are available in supplementary material.

The mass transfer coefficient  $k_L a$  was determined at different agitation rates, from 300 to 1500 rpm, with a maximum obtained at 1000 rpm. This rate was therefore chosen as an operating parameter for the biomethanation reactor.

The mass transfer coefficients of  $H_2$  and  $CO$  in water were then computed from the mass transfer coefficient of  $O_2$  using the diffusivities ratio according to Eq. 4:

$$k_L a_i = k_L a_{O_2} \left( \frac{D_i}{D_{O_2}} \right)^{0.5} \quad (4)$$

The square roots of the diffusivities ratios  $(D_i/D_{O_2})^{0.5}$  was computed according to correlations determined by Wilke and Chang (1955). They were found to be 1.22 and 0.97 for  $H_2$  and  $CO$ , respectively.

### 2.3 Calculation methods

All kinetic parameters were estimated for a single inlet syngas flow rate, during a stable period of methane production. The uncertainties were computed from the standard deviations calculated for each period, using the propagation of uncertainty method. A minimum of 12 data was used to calculate the standard deviation for each period. Moreover, for each period, mass balances between the inlet and the outlet of the reactor were calculated to validate the conservation of mass in the system (data not shown).

For each syngas inflow rate, the corresponding conversion rates and productivities  $r$  ( $L_{STP}/L/d$ ) were measured with the same method as described in Figueras et al. (2021). The specific rates  $r_x$  ( $L_{STP}/g_{VS}/d$ ) were calculated with the volatile suspended solids concentration. Since VS content was not measured at the beginning and the end of each syngas inflow rate steps, those points were obtained with linear approximation from the measured VS concentration and used to compute the mean VS concentration for each syngas inflow rate step. In order for the VS concentration to be a

better estimate of biomass growth, it was corrected for acid volatile concentrations according to Porter and Murray (2001).

The maximum mass transfer rate  $N_{\max,i}$  ( $L_{\text{STP}}/L/d$ ) of a component  $i$  is computed according to Eq. 5:

$$N_{\max,i} = k_{L,i}(Q_{\text{total}}) * H_{i, \text{cp}} * P_i \quad (5)$$

$k_{L,i}$  is the mass transfer coefficient of  $i$  ( $1/d$ ) and depends on the total actual flow rate  $Q_{\text{total}}$ . The correlation between the  $k_{L,i}$  and  $Q_{\text{total}}$  was determined during the mass transfer characterization (supplementary material).

During the process, according to Eq. 1 and 2, the number of moles of gaseous components tends to decrease. With a syngas composed of 40% CO, 40% H<sub>2</sub> and 20% CO<sub>2</sub>, assuming total conversion, the outlet dry gas would be composed of 33% CH<sub>4</sub> and 67% CO<sub>2</sub> and the outlet flow rate would be only 60% of the injected flow rate. According to Eq. 5, the maximum mass transfer rate depends on the actual gas flow rate (impact on the  $k_{L,i}$ ) and on the partial pressure of the considered gas.

For example, with a CO partial pressure at the entrance of the reactor set at 1.6 bar, the CO outlet partial pressure was found to be equal to 0.1 bar during stable methanogenesis at 4 bar and for 18  $L_{\text{STP, syngas}}/L/d$ .

The average values of these two parameters (gas flow rate and partial pressure) depend on the mixing behaviour of the gas phase. Two models can be considered. The first model assumes that the gas phase is perfectly mixed: bubbles are homogeneously distributed, and the composition of the gas phase is homogeneous and equal to the outlet composition (Continuous Stirred Tank Reactor (CSTR) model). In this case, it is considered that the parameters impacting the transfer are the outlet flow rate and outlet partial pressure. The second model considers that the gas phase behaves as plug flow reactor (PFR) system. In this case, there is a gradient of gas composition and

gas flow rate between the entrance and the exit of the reactor. Under this assumption, the average flow rate ( $Q_{global}$ ) and partial pressure ( $P_i$ ) impacting the mass transfer rates are computed using the logarithmic mean between the entrance (in) and the exit (out) of the reactor (Villadsen et al., 2011):

$$P_i^{log} = \frac{P_i^{in} - P_i^{out}}{\ln(P_i^{in}) - \ln(P_i^{out})} [bar], \quad (6)$$

$$Q_{global}^{log} = \frac{Q_{global}^{in} - Q_{global}^{out}}{\ln(Q_{global}^{in}) - \ln(Q_{global}^{out})} [L/h] \quad (7)$$

In reality, the actual behaviour of the gas phase probably lies between these two extreme models (Danckwerts, 1995). In a bubble column (without mechanical mixing), the gas phase is generally assumed to behave as a plug flow system. The residence time distribution of the gas, measured with an inert tracer, could allow to determine the real behaviour of the system (Rodrigues, 2021). However, it was not possible to measure it in this study due to lack of the appropriate equipment. Therefore, it was decided to consider the two extreme models (PFR and CSTR) to discuss the mass transfer of the reactor.

### 3 Results and discussion

#### 3.1 Biomethanation performances

The performance parameters of biomethanation depending on the syngas inflow rate are presented in Fig. 2, for experiment A and B. Even though the two experiments were conducted a few months apart, the results are quite similar indicating a good reproducibility of the biological process. Therefore, it can be observed that the duration time of each inflow rate step had no impact on the performance results. It can also be seen in Fig. 2 that a 20% increase in syngas flow rate led to a quick stabilisation of the outlet flow rate, with no apparent transient state. This tends to indicate that the process was not limited by biological kinetics. It can also be noted in Fig. 2 the

presence of residual H<sub>2</sub> and CO flow rates, that increased with the increase of syngas inflow rate. This also indicates mass transfer limitations. Because stable performances established quickly as the flow rates changed, it was possible to characterize performances in steady state.

Considering the by-products of biomethanation, presence of volatile fatty acid (VFA) was detected, mostly acetic and propionic acid. In Experiment A, VFA concentrations ranged around 0.1 mg/L and 0.5 mg/L for acetic and propionic acid respectively (Fig. 2), whereas they were much higher in experiment B (around 3-2 g/L). This higher concentration didn't seem to inhibit biomethanation as the volumetric conversion rates and productivities were similar between experiment A and B (Fig. 3). In both experiments, the acetic acid concentrations decreased over time (from 0.4 to  $0.003 \pm 5\%$  g/L for experiment A and from 3.8 to  $1.4 \pm 5\%$  g/L for experiment B). This trend has already been observed in a previous study (Figueras et al., 2021), with an increase in acetic acid concentration when methanogenesis was inhibited, and a decrease when methanogenesis was occurring. This indicates that acetic acid is probably a by-product when methanogenesis is limited, and not when it is thriving.

During the experiments, VS concentration increased, which is due to biomass growth. In Experiment A, VS concentration increased of  $2.2 \pm 0.2$  g/L in 15 days and in Experiment B, of  $3.9 \pm 0.2$  g/L in 4 days. Therefore, biomass growth was more important and quicker in Experiment B compared to Experiment A. As mentioned in 2.1, sulfur supply was increased in Experiment B compared to Experiment A, which could have favoured biomass growth.

From the data obtained at steady states at each syngas inflow rates tested, conversion rates and productivities were calculated for experiment A and B and are displayed in Fig. 3. One can observe that the volumetric conversion rate of H<sub>2</sub> ( $r_{H_2}$ ) was almost twice higher than the volumetric conversion rate of CO ( $r_{CO}$ ). This makes sense, as  $r_{H_2}$  is computed by considering the H<sub>2</sub> produced

from CO by water-gas shift according to Eq. 1 (Figueras et al., 2021). It can also be observed that the volumetric production and conversion rates increased with the syngas inflow rate. An outlet production rate of  $23.2 \pm 0.2 \text{ L}_{\text{CH}_4}/\text{L}/\text{d}$  was reached for a maximum inlet syngas flow rate tested of  $135.6 \text{ L}_{\text{STP}}/\text{L}/\text{d}$ .

At the lower syngas inflow rate of  $18.0 \text{ L}_{\text{STP}}/\text{L}/\text{d}$ , the CO conversion efficiencies ( $E_{\text{CO}}$ ) were of  $96 \pm 0\%$  for experiment A and of  $97 \pm 0\%$  for experiment B. At the maximum inflow rate of  $135.6 \text{ L}_{\text{STP}}/\text{L}/\text{d}$ , they dropped to  $82 \pm 1\%$  and  $79 \pm 1\%$  for experiments A and B, respectively. The same tendency can be observed regarding  $\text{H}_2$  conversion efficiencies ( $E_{\text{H}_2}$ ). The drop in conversion efficiencies can be explained by the decrease of the gas retention time associated with an increase in the inflow rate. Such behaviour has already been observed in syngas biomethanation (Asimakopoulos et al., 2021b).

It can also be observed in Fig. 4 that  $E_{\text{H}_2}$  was always higher than  $E_{\text{CO}}$ . This can be explained by  $\text{H}_2$  mass transfer properties, that are slightly higher than CO mass transfer properties. Indeed, as mentioned in 2.2, the square roots of the diffusivities ratio for  $\text{H}_2$  (1.22) is higher than for CO (0.97), indicating a higher  $k_{\text{La}}$  for  $\text{H}_2$  compared to CO (Eq. 4). Moreover, at  $55^\circ\text{C}$  the Henry law coefficient for  $\text{H}_2$  is  $6.63 \cdot 10^{-6} \text{ mol}/(\text{m}^3 \cdot \text{Pa})$  and  $6.52 \cdot 10^{-6} \text{ mol}/(\text{m}^3 \cdot \text{Pa})$  for CO, according to Sander (2015). Therefore, according to Eq. 5, the overall mass transfer rate of  $\text{H}_2$  is higher than the overall mass transfer rate of CO.

Comparing performances obtained in this study to literature is a complex task, as the parameters vary widely from one study to the other. Moreover, the mass transfer is not always characterized, hence making it difficult to compare the performances between different studies. When comparing the methane productivities, a few parameters must be considered. The methane productivity tends

to increase with the syngas inflow rate, although often at the expense of the conversion efficiencies. Therefore, one should also consider the mass transfer efficiency.

Moreover, the syngas composition will influence the methane composition of the outlet gas, according to Eq. 1 and 2. The syngas quality index (SQI) was introduced by Asimakopoulos et al. (2021a) and is useful to compare performances of different processes converting different syngas compositions. The more the SQI (Eq. 8) tends to 4, the higher the methane content in the produced gas.

$$SQI = \frac{\%H_2 + \%CO}{\%CO_2 + \%CO} \quad (8)$$

Taking these parameters into account, at similar inflow rates per unit of reactor volume and temperature conditions, performances can be compared between two studies. For example, in this study, a syngas inflow rate of 64.8 L<sub>STP</sub>/L/d was tested, which is close to a syngas inflow rate tested by Asimakopoulos et al. (2021b) of 65.8 L<sub>STP</sub>/L/d using a trickle bed reactor at atmospheric pressure. Even though their syngas flow rate per unit of reactor volume and SQI (1.44) were higher compared to this study (with SQI of 1.33), they obtained lower methane productivity (9.5 L<sub>STP</sub>/L/d) compared to this study (11.8 ± 0.1 L<sub>STP</sub>/L/d). This can be explained by the difference of conversion efficiencies (76% and 97% for their study and 88% and 94% for this study, for CO and H<sub>2</sub> respectively), which can be explained by the mass transfer technologies used: it could be hypothesized that working at high pressure tends to increase the mass-transfer capacity of the reactor.

Considering methane productivity data from the literature, the highest methane productivity obtained in the literature prior to this study was 9.5 L<sub>STP, CH4</sub>/L/d, obtained by Asimakopoulos et al. (2021b) as described above. Other performances can be mentioned, such as 4.6 L<sub>STP, CH4</sub>/L/d (E<sub>CO</sub>: 73%, E<sub>H2</sub>: 89%) by Asimakopoulos et al. (2020), 3.6 L<sub>STP, CH4</sub>/L/d (E<sub>CO</sub>: 93%, E<sub>H2</sub>: 97%) by Diender et al.

(2018) and  $3.7 \text{ L}_{\text{STP, CH}_4}/\text{L}/\text{d}$  ( $E_{\text{CO}}$ : 97%,  $E_{\text{H}_2}$ : 98%) by Figueras et al. (2021). Therefore, to our knowledge, the highest methane productivity of  $23.2 \text{ L}_{\text{STP, CH}_4}/\text{L}/\text{d}$  obtained in this study is the highest volumetric methane productivity achieved yet with syngas biomethanation. This is probably because it is the first time that such a high syngas inflow rate ( $135.6 \text{ L}_{\text{STP}}/\text{L}/\text{d}$ ) was applied. There are not yet other studies working at such an inflow rate allowing to compare these performances. Even though the corresponding conversion efficiencies obtained with  $23.2 \text{ L}_{\text{CH}_4}/\text{L}/\text{d}$  are around 82-79% for  $E_{\text{CO}}$  and 89-87% for  $E_{\text{H}_2}$  and are not suitable for network gas injection, the performances obtained in this study are very promising for syngas biomethanation since they could still be improved by improving the mass transfer rate. To do this, simple reactor geometry changes could be implemented, such as adding baffles to the tank and therefore increasing mass transfer rate (Cabaret et al., 2008). Another solution, when designing the tank would be choosing for a similar working volume a higher height/diameter ratio that would allow for longer gas residence time and therefore increase the mass transfer.

### 3.2 Mass transfer study

Mass transfer is a known limiting factor of biomethanation (Asimakopoulos et al., 2018). As pressure can increase gas solubility and therefore the mass transfer rate according to Eq. 5, a pressurized stirred bubble column reactor was implemented. However, in gas sparged reactor, pressure can also reduce the  $k_{\text{L}}a$  as it decreases the gas volume and therefore the bubble size and the interfacial area (Jensen et al., 2021). To confirm that pressure had a positive impact on the overall maximum mass transfer rate, the performances of the reactor were investigated for a fixed inlet syngas flow rate of  $18.0 \text{ L}_{\text{STP}}/\text{L}/\text{d}$  at 1 and 4 bar for experiment A.

By increasing the pressure, the CO conversion rate increased by 12%, from  $6.1 \pm 0.3$  to  $6.9 \pm 0.1 \text{ L}/\text{L}/\text{d}$ . Similarly, the methane productivity increased by 12% from  $3.1 \pm 0.1$  to  $3.5 \pm 0.1 \text{ L}/\text{L}/\text{d}$ .

Moreover, the conversion efficiencies increased from  $85 \pm 4 \%$  to  $96 \pm 0 \%$  for CO (11% increase) and from  $89 \pm 3 \%$  to  $97 \pm 0 \%$  for H<sub>2</sub> (9% increase) when increasing the reactor pressure. These results confirm the positive impact of pressure on the mass transfer.

As mentioned earlier, the volumetric rates were very similar between experiment A and B. However, the VS concentrations in experiments A and B were quite different ( $5.4 \pm 0.1$  g/L and  $6.8 \pm 0.1$  g/L). Therefore, specific activities were computed. Their evolution according to syngas inflow rates are displayed in Fig. 3. It can be observed that the specific activities also increased with the syngas inflow rate. However, contrary to the volumetric conversion and production rates, the specific activities were different between experiment A and B. The specific activities in experiment B were lower than of experiment A, as the VS concentration was higher in experiment B. Since the volumetric rates were similar for experiment A and B, and since the specific activities were different, this indicates that the reactor was limited by mass transfer and not by biological kinetics. Considering the two different models discussed in 2.3, the theoretical maximal mass transfer rates were computed considering a CSTR model and a PFR model for the gas phase. These theoretical maximal mass transfer rates were then compared to the observed volumetric conversion rates. To study mass transfer performances, only the carbon monoxide mass transfer was considered, as it is not considered an intermediary product of the process (on the contrary to H<sub>2</sub> that is at the same time injected in the reactor and produced by the water gas shift reaction from CO).

It can be observed in Fig. 5 that for experiment A the volumetric conversion rate for CO was higher than the theoretical  $N_{\max}$ , independently of the model considered and significantly when comparing to the uncertainties computed as described in Material and Method. This is surprising: since it is considered that the reactor is transfer limited, the opposite result should be observed. The  $N_{\max}$  computed with the PFR model was higher than the  $N_{\max}$  computed with the CSTR model, which

makes sense as the CSTR model only considers the outlet CO partial pressure ( $P_{CO}^{out}$ ), which is smaller than the logarithmic partial pressure ( $P_{CO}^{log}$ ) considered in the PFR model. For example, for experiment B at  $135.6 \text{ L}_{STP, \text{ syngas}}/\text{L}/\text{d}$ ,  $P_{CO}^{out}$  was equal to  $0.48 \pm 0.02 \text{ bar}$  and  $P_{CO}^{log}$  was equal to  $0.93 \pm 0.02 \text{ bar}$ . According to Eq. 5, the higher the gas partial pressure the higher the mass transfer rate, hence explaining the better performances of the PFR model.

According to these results, it can be concluded that the CO mass transfer under process conditions is faster than without biological reaction. This difference is quantified by an enhancement factor  $Ea$ , computed according to Eq. 9:

$$Ea = r_{CO} / N_{max} \quad (9)$$

Mass transfer enhancement in gas-liquid reactive systems is a known phenomenon. According to the two film theory for gas-liquid mass transfer (Lewis and Whitman, 1924), it occurs when the reaction takes place (partly or totally) in the liquid film diffusion layer at the gas-liquid interface. This is due to the fact that the reaction rate is faster than the diffusion rate (Kierzkowska-Pawlak, 2012).

Considering that the biological process of this study is transfer limited as argued above, an analogy can be made with mass transfer with chemical reaction to explain the observed enhancement factor. This has been already proposed by several studies, that observed and modelled a biological enhancement factor for the biological oxygen uptake (Merchuk, 1977; Garcia-Ochoa and Gomez, 2005, 2009).

Merchuk (1977) considered a mono film model and modelled the concentration gradient of oxygen through the liquid film. They demonstrated that the enhancement factor could be expressed as:

$$Ea = 1 + \left( \frac{D \cdot r_x \cdot X}{2 \cdot k_l^2 \cdot (C^* - C_l)} \right) \quad (11)$$

With  $D$  the gas diffusivity ( $\text{cm}^2/\text{d}$ ),  $(C^* - C_L)$  the dissolved gas concentration gradient ( $L_{\text{STP}}/L$ ),  $k_L$  the liquid-side mass transfer coefficient ( $\text{cm}/\text{d}$ ),  $r_x$  the specific activity ( $L_{\text{STP}}/\text{g}_{\text{VS}}/\text{d}$ ) and  $X$  the biomass concentration ( $\text{g}_{\text{VS}}/L$ ). They demonstrated that the enhancement factor was dependent on the cell concentration and distribution in the liquid film. Furthermore, Garcia-Ochoa and Gomez (2005) proposed a model considering mass transfer resistances in series (surfactant layer, cell layer, liquid film layer). They also concluded that the biological enhancement factor was dependent on the conversion rate (which depends on the specific activity and the biomass concentration), with good correlation with experimental observations.

Therefore, in this study, the evolution of the biological enhancement factor with the CO conversion rates was considered, for each steady states at constant syngas inflow rates. The increase in the enhancement factor with the volumetric conversion rate can indeed be noticed in Fig. 6, considering the PFR model. More than a two-time increase can be observed, from around 1.5 to 3.2. This increasing trend is in accordance with the modeling proposed by the studies as discussed above. However, these values are quite high compared to literature: for example, Garcia-Ochoa and Gomez (2009) observed a biological enhancement factor ranging from 1 to 1.3 for the growth of a pure culture of *Candida bombicola* in a stirred tank reactor. The values for  $E_a$  are similar in experiments A and B for the PFR model. Considering the CSTR model for the gas phase, the values are much higher, with  $E_a$  ranging from about 6 to 13. In addition, the values are much more scattered between experiment A and B. No clear trend can be extrapolated for  $E_a$ . Even if the real mass transfer behaviour would probably be between the CSTR and the PFR model (Danckwerts, 1995), this observation leads to think that the mass transfer model probably leans toward a PFR model. This would be consistent with the fact that the gas phase in the system is composed of fine individual rising bubbles, even if the mixing intensity is elevated.

To our knowledge, it is the first time that a biological enhancement factor is observed in a biomethanation process. Modelling of the concentration profile of CO in the liquid film to determine theoretical values for the enhancement factor and comparing them with the trend observed Fig.6 would provide more in depth understanding of the mechanisms, which could be the aim of further research.

## 4 Conclusion

For the first time, high syngas inflow rate conversion was tested with biomethanation with two strategies of syngas flow rates increase. High methane productivity of 23.2 L<sub>CH<sub>4</sub></sub>/L/d was obtained, associated with good conversion efficiencies of 89% for H<sub>2</sub> and 82% for CO. Using a pressurized reactor to improve gas-liquid mass transfer led to good performances compared to the literature. Therefore, these results are a good step towards the industrialization of the process. When studying the mass transfer performances of the reactor, the existence of a biological enhancement factor was demonstrated. Future work should investigate the mechanisms governing this phenomenon.

E-supplementary data for this work can be found in e-version of this paper online.

## Declaration of Competing Interest

The authors declare that they have no known competing financial interests or personal relationships that could have appeared to influence the work reported in this paper.

## Acknowledgements

The authors would like to thank ENOSIS for the financial support, Richard Poncet and Hervé Périer-Camby for the original experimental setup, Nathalie Dumont and David Le Bouil for the chemical

analysis. This work was performed within the framework of the EUR H2O'Lyon (ANR-17-EURE-0018) of Université de Lyon (UdL), within the program "Investissements d'Avenir" operated by the French National Research Agency (ANR)

## Funding

This work was supported by the Association Nationale de la Recherche et de la Technologie and the company ENOSIS. The funding sources had no involvement in study design; in the collection, analysis and interpretation of data; in the writing of the report; and in the decision to submit the article for publication.

## References

1. Arena, U., 2012. Process and technological aspects of municipal solid waste gasification. A review. *Waste Management* 32, 625–639. <https://doi.org/10.1016/j.wasman.2011.09.025>
2. Aryal, N., Odde, M., Bøgeholdt Petersen, C., Ditlev Mørck Ottosen, L., Vedel Wegener Kofoed, M., 2021. Methane production from syngas using a trickle-bed reactor setup. *Bioresource Technology* 333, 125183. <https://doi.org/10.1016/j.biortech.2021.125183>
3. Asimakopoulos, K., 2019. Biomethanation of synthesis gas in trickle bed reactors.
4. Asimakopoulos, K., Gavala, H.N., Skiadas, I.V., 2018. Reactor systems for syngas fermentation processes: A review. *Chemical Engineering Journal* 348, 732–744. <https://doi.org/10.1016/j.cej.2018.05.003>
5. Asimakopoulos, K., Grimalt-Alemany, A., Lundholm-Høffner, C., Gavala, H.N., Skiadas, I.V., 2021a. Carbon Sequestration Through Syngas Biomethanation Coupled with H<sub>2</sub> Supply for a Clean Production of Natural Gas Grade Biomethane. *Waste Biomass Valor.* <https://doi.org/10.1007/s12649-021-01393-2>

6. Asimakopoulos, K., Kaufmann-Elfang, M., Lundholm-Høffner, C., Rasmussen, N.B.K., Grimalt-Alemany, A., Gavala, H.N., Skiadas, I.V., 2021b. Scale up study of a thermophilic trickle bed reactor performing syngas biomethanation. *Applied Energy* 290, 116771.  
<https://doi.org/10.1016/j.apenergy.2021.116771>
7. Asimakopoulos, K., Łężykb, M., Grimalt-Alemany, A., Melas, A., Wen, Z., Gavala, H.N., Skiadas, I.V., 2020. Temperature effects on syngas biomethanation performed in a trickle bed reactor. *Chemical Engineering Journal* 13.
8. Cabaret, F., Fradette, L., Tanguy, P.A., 2008. Gas–liquid mass transfer in unbaffled dual-impeller mixers. *Chemical Engineering Science* 63, 1636–1647. <https://doi.org/10.1016/j.ces.2007.11.028>
9. Danckwerts, P.V., 1995. Continuous flow systems. Distribution of residence times. *Chemical Engineering Science, Frontiers of Chemical Engineering Science* 50, 3857–3866.  
[https://doi.org/10.1016/0009-2509\(96\)81811-2](https://doi.org/10.1016/0009-2509(96)81811-2)
10. Diender, M., Uhl, P.S., Bitter, J.H., Stams, A.J.M., Sousa, D.Z., 2018. High Rate Biomethanation of Carbon Monoxide-Rich Gases via a Thermophilic Synthetic Coculture. *ACS Sustainable Chemistry & Engineering* 6, 2169–2176. <https://doi.org/10.1021/acssuschemeng.7b03601>
11. Dolk, H., Vrijheid, M., Armstrong, B., Abramsky, L., Bianchi, F., Garne, E., Nelen, V., Robert, E., Scott, J., Stone, D., Tenconi, R., 1998. Risk of congenital anomalies near hazardous-waste landfill sites in Europe: the EUROHAZCON study. *The Lancet* 352, 423–427.  
[https://doi.org/10.1016/S0140-6736\(98\)01352-X](https://doi.org/10.1016/S0140-6736(98)01352-X)
12. Figueras, J., Benbelkacem, H., Dumas, C., Buffiere, P., 2021. Biomethanation of syngas by enriched mixed anaerobic consortium in pressurized agitated column. *Bioresource Technology* 338, 125548. <https://doi.org/10.1016/j.biortech.2021.125548>

13. Garcia-Ochoa, F., Gomez, E., 2009. Bioreactor scale-up and oxygen transfer rate in microbial processes: An overview. *Biotechnology Advances* 27, 153–176.  
<https://doi.org/10.1016/j.biotechadv.2008.10.006>
14. Garcia-Ochoa, F., Gomez, E., 2005. Prediction of gas-liquid mass transfer coefficient in sparged stirred tank bioreactors. *Biotechnol. Bioeng.* 92, 761–772. <https://doi.org/10.1002/bit.20638>
15. Grimalt-Alemany, A., Łężyk, M., Kennes-Veiga, D.M., Skiadas, I.V., Gavala, H.N., 2019. Enrichment of Mesophilic and Thermophilic Mixed Microbial Consortia for Syngas Biomethanation: The Role of Kinetic and Thermodynamic Competition. *Waste Biomass Valor.*  
<https://doi.org/10.1007/s12649-019-00595-z>
16. Grimalt-Alemany, A., Skiadas, I.V., Gavala, H.N., 2018. Syngas biomethanation: state-of-the-art review and perspectives. *Biofuels, Bioproducts and Biorefining* 12, 139–158.
17. Guiot, S.R., Cimpoaia, R., Carayon, G., 2011. Potential of Wastewater-Treating Anaerobic Granules for Biomethanation of Synthesis Gas. *Environmental Science & Technology* 45, 2006–2012.  
<https://doi.org/10.1021/es102728m>
18. He, Z., Petiraksakul, A., Meesapaya, W., 2003. Oxygen-Transfer Measurement in Clean Water 13, 6.
19. Jensen, M.B., Ottosen, L.D.M., Kofoed, M.V.W., 2021. H<sub>2</sub> gas-liquid mass transfer: A key element in biological Power-to-Gas methanation. *Renewable and Sustainable Energy Reviews* 147, 111209. <https://doi.org/10.1016/j.rser.2021.111209>
20. Kierzkowska-Pawlak, H., 2012. Determination of Kinetics in Gas-Liquid Reaction Systems. An Overview. *Ecological Chemistry and Engineering S* 19, 175–196. <https://doi.org/10.2478/v10216-011-0014-y>
21. Lewis, W.K., Whitman, W.G., 1924. Principles of Gas Absorption. *Ind. Eng. Chem.* 16, 1215–1220.  
<https://doi.org/10.1021/ie50180a002>

22. Li, C., Zhu, X., Angelidaki, I., 2021. Syngas biomethanation: effect of biomass-gas ratio, syngas composition and pH buffer. *Bioresource Technology* 342, 125997.  
<https://doi.org/10.1016/j.biortech.2021.125997>
23. Li, C., Zhu, X., Angelidaki, I., 2020. Carbon monoxide conversion and syngas biomethanation mediated by different microbial consortia. *Bioresource Technology* 9.
24. Li, Y., Liu, Y., Wang, X., Luo, S., Su, D., Jiang, H., Zhou, H., Pan, J., Feng, L., 2022. Biomethanation of syngas at high CO concentration in a continuous mode. *Bioresource Technology* 346, 126407.  
<https://doi.org/10.1016/j.biortech.2021.126407>
25. Li, Y., Su, D., Luo, S., Jiang, H., Qian, M., Zhou, H., Street, J., Luo, Y., Xu, Q., 2017. Pyrolysis gas as a carbon source for biogas production via anaerobic digestion. *RSC Advances* 7, 41889–41895.  
<https://doi.org/10.1039/C7RA08559A>
26. Li, Y., Wang, Z., He, Z., Luo, S., Su, D., Jiang, H., Zhou, H., Xu, Q., 2019. Effects of temperature, hydrogen/carbon monoxide ratio and trace element addition on methane production performance from syngas biomethanation. *Bioresource Technology* 122296.  
<https://doi.org/10.1016/j.biortech.2019.122296>
27. Merchuk, J.C., 1977. Further considerations on the enhancement factor for oxygen absorption into fermentation broth. *Biotechnol. Bioeng.* 19, 1885–1889.  
<https://doi.org/10.1002/bit.260191211>
28. Palmiotto, M., Fattore, E., Paiano, V., Celeste, G., Colombo, A., Davoli, E., 2014. Influence of a municipal solid waste landfill in the surrounding environment: Toxicological risk and odor nuisance effects. *Environment International* 68, 16–24.  
<https://doi.org/10.1016/j.envint.2014.03.004>
29. Porter, M.G., Murray, R.S., 2001. The volatility of components of grass silage on oven drying and the inter-relationship between dry-matter content estimated by different analytical methods:

- Inter-relationships between estimates of silage dry matter. *Grass and Forage Science* 56, 405–411. <https://doi.org/10.1046/j.1365-2494.2001.00292.x>
30. Pradhan, A., Baredar, P., Kumar, A., 2015. Syngas as An Alternative Fuel Used in Internal Combustion Engines: A Review 5, 16.
31. Ren, J., Liu, Y.-L., Zhao, X.-Y., Cao, J.-P., 2020. Methanation of syngas from biomass gasification: An overview. *International Journal of Hydrogen Energy* 45, 4223–4243. <https://doi.org/10.1016/j.ijhydene.2019.12.023>
32. Rodrigues, A.E., 2021. Residence time distribution (RTD) revisited. *Chemical Engineering Science* 230, 116188. <https://doi.org/10.1016/j.ces.2020.116188>
33. Sander, R., 2015. Compilation of Henry's law constants (version 4.0) for water as solvent. *Atmos. Chem. Phys.* 15, 4399–4981. <https://doi.org/10.5194/acp-15-4399-2015>
34. Sipma, J., Lens, P.N.L., Stams, A.J.M., Lettinga, G., 2003. Carbon monoxide conversion by anaerobic bioreactor sludges. *FEMS Microbiology Ecology* 44, 271–277. [https://doi.org/10.1016/S0168-6496\(03\)00033-3](https://doi.org/10.1016/S0168-6496(03)00033-3)
35. Tanigaki, N., Ishida, Y., Osada, M., 2015. A case-study of landfill minimization and material recovery via waste co-gasification in a new waste management scheme. *Waste Management* 37, 137–146. <https://doi.org/10.1016/j.wasman.2014.07.024>
36. Tsui, T.-H., Wong, J.W.C., 2019. A critical review: emerging bioeconomy and waste-to-energy technologies for sustainable municipal solid waste management. *Waste Dispos. Sustain. Energy* 1, 151–167. <https://doi.org/10.1007/s42768-019-00013-z>
37. Vehlow, J., Bergfeldt, B., Visser, R., Wilén, C., 2007. European Union waste management strategy and the importance of biogenic waste. *J Mater Cycles Waste Manag* 9, 130–139. <https://doi.org/10.1007/s10163-007-0178-9>

38. Villadsen, J., Nielsen, J., Lidén, G., 2011. Gas–Liquid Mass Transfer, in: Bioreaction Engineering Principles. Springer US, Boston, MA, pp. 459–496. [https://doi.org/10.1007/978-1-4419-9688-6\\_10](https://doi.org/10.1007/978-1-4419-9688-6_10)
39. Westman, S., Chandolias, K., Taherzadeh, M., 2016. Syngas Biomethanation in a Semi-Continuous Reverse Membrane Bioreactor (RMBR). *Fermentation* 2, 8. <https://doi.org/10.3390/fermentation2020008>
40. Wilke, C.R., Chang, P., 1955. Correlation of diffusion coefficients in dilute solutions. *AIChE J.* 1, 264–270. <https://doi.org/10.1002/aic.690010222>
41. Youngsukkasem, S., Chandolias, K., Taherzadeh, M.J., 2015. Rapid bio-methanation of syngas in a reverse membrane bioreactor: Membrane encased microorganisms. *Bioresource Technology* 178, 334–340. <https://doi.org/10.1016/j.biortech.2014.07.071>

## Figures Captions

Fig. 1. Schematic of the reactor system. (1) tank, (2) stirring system, (3) pressurized sulfide circuit, (4) thermostat, (5) CO gas bottle, (6) CO mass flow controller, (7) CO<sub>2</sub> gas bottle, (8) CO<sub>2</sub> mass flow controller, (9) H<sub>2</sub> generator, (10) H<sub>2</sub> mass flow controller, (11) liquid addition or withdraw, (12) pressure controller, (13) gas analyzer, (14) drum gas counter.

Fig. 2. Evolution of syngas inflow rate, of outlet flow rates and of the by-products of biomethanation in function of time, for experiments A and B. In experiment A, the syngas inflow rate was increased by 20% every 24h, whereas in experiment B it was increased every 3h. Every 3 to 4 days, the reactor was depressurized, and liquid sampling was performed to measure volatile solids (VS) and volatile fatty acid (VFA) concentrations. VS concentrations are corrected for VFA. In Experiment A, the CO inflow rate was interrupted from day 10.4 to day 12, due to the emptying of the CO bottle. The experiment restarted day 12 with no visible impact of the biomethanation.

Fig. 3. Evolution of CO and H<sub>2</sub> volumetric conversion rates, volumetric CH<sub>4</sub> production rate, and specific activities for H<sub>2</sub> and CO conversion, and for CH<sub>4</sub> production in function of the syngas inflow rate, for experiments A and B.

Fig. 4 Drop of conversion efficiencies with the increase in syngas inflow rate. E<sub>CO</sub>: CO conversion efficiency, E<sub>H<sub>2</sub></sub>: H<sub>2</sub> conversion efficiency.

Fig. 5 Comparison of CO volumetric conversion rates ( $r_{CO}$ ) and CO maximal mass transfer rates ( $N_{maxCO}$ ), considering Continuous Stirred Tank Reactor (CSTR) and Plug Flow Reactor (PFR) transfer models.

Fig. 6 Evolution of the biological enhancement factor in function of CO conversion rate, for experiments A and B, considering a Continuous Stirred Tank Reactor (CSTR) and Plug Flow Reactor (PFR) model.

# Tables and Figures

Figure 1

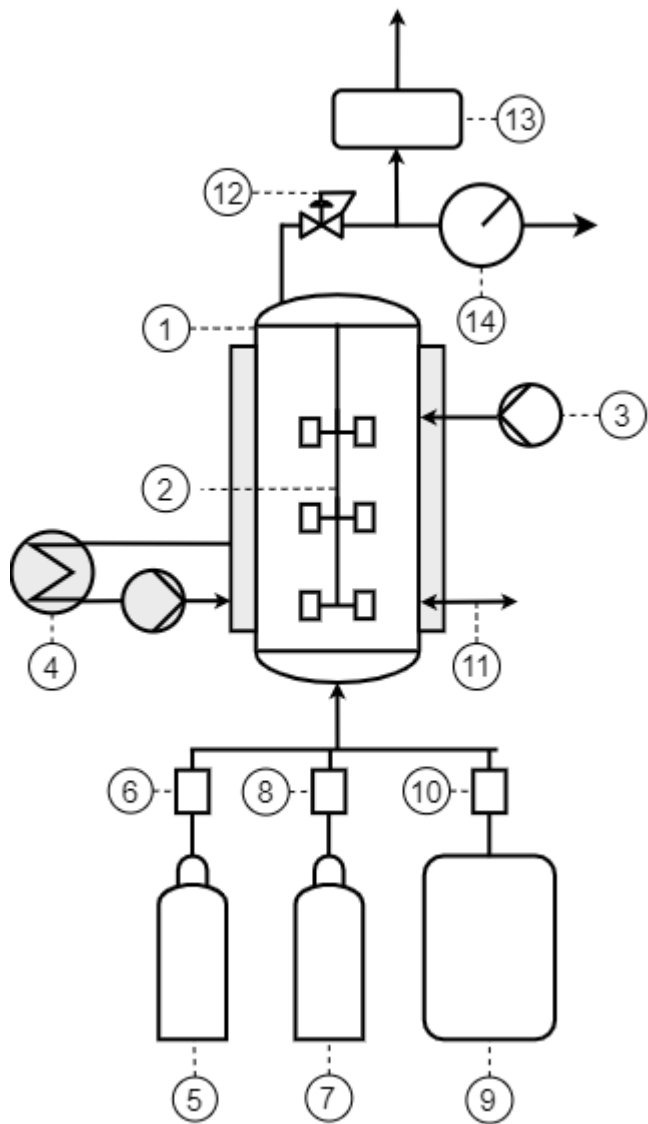


Figure 2

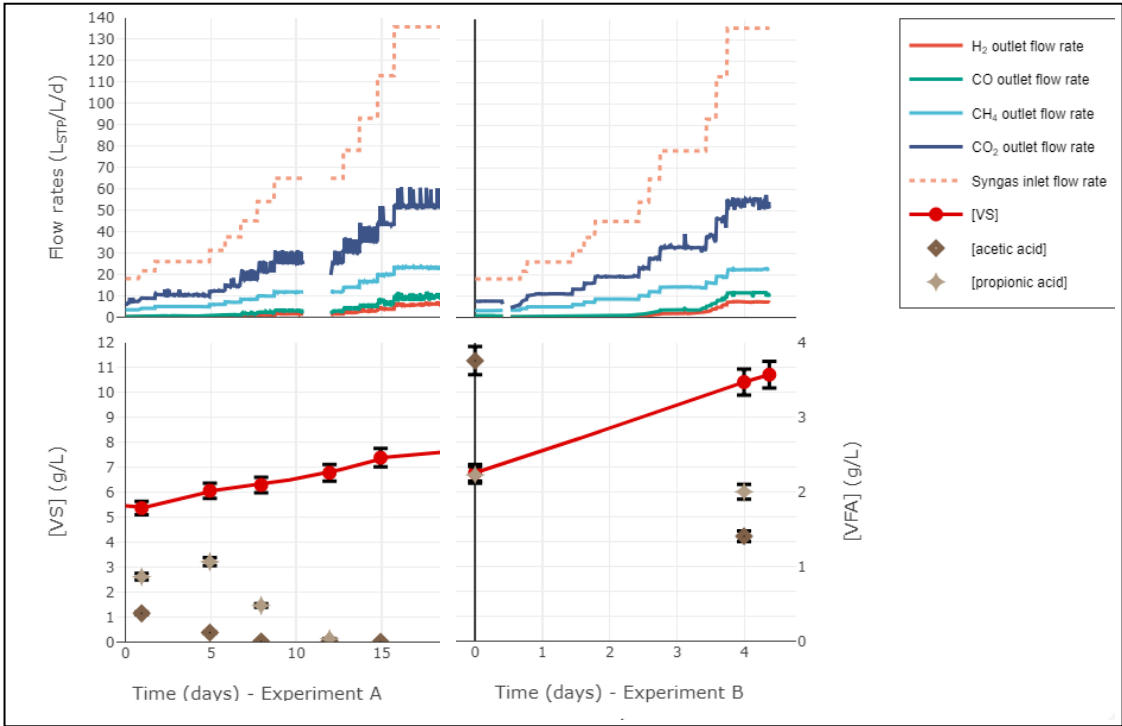


Figure 3

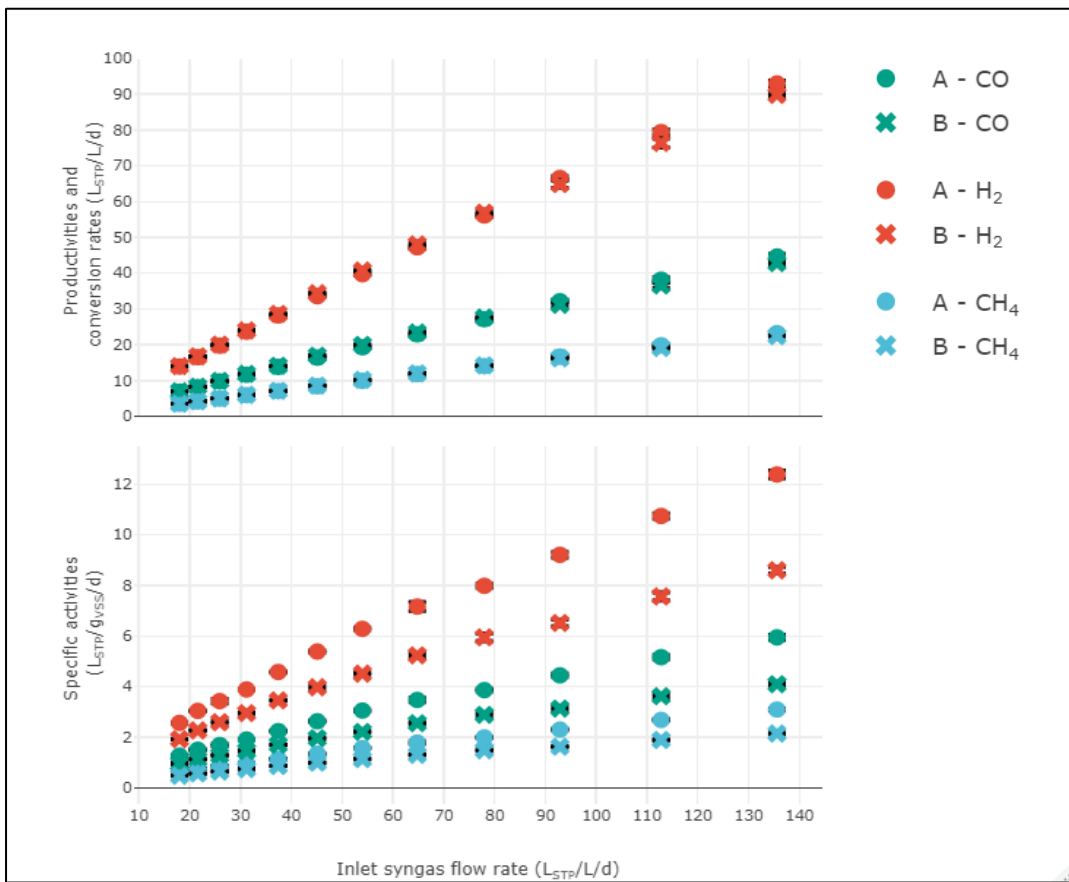


Figure 4

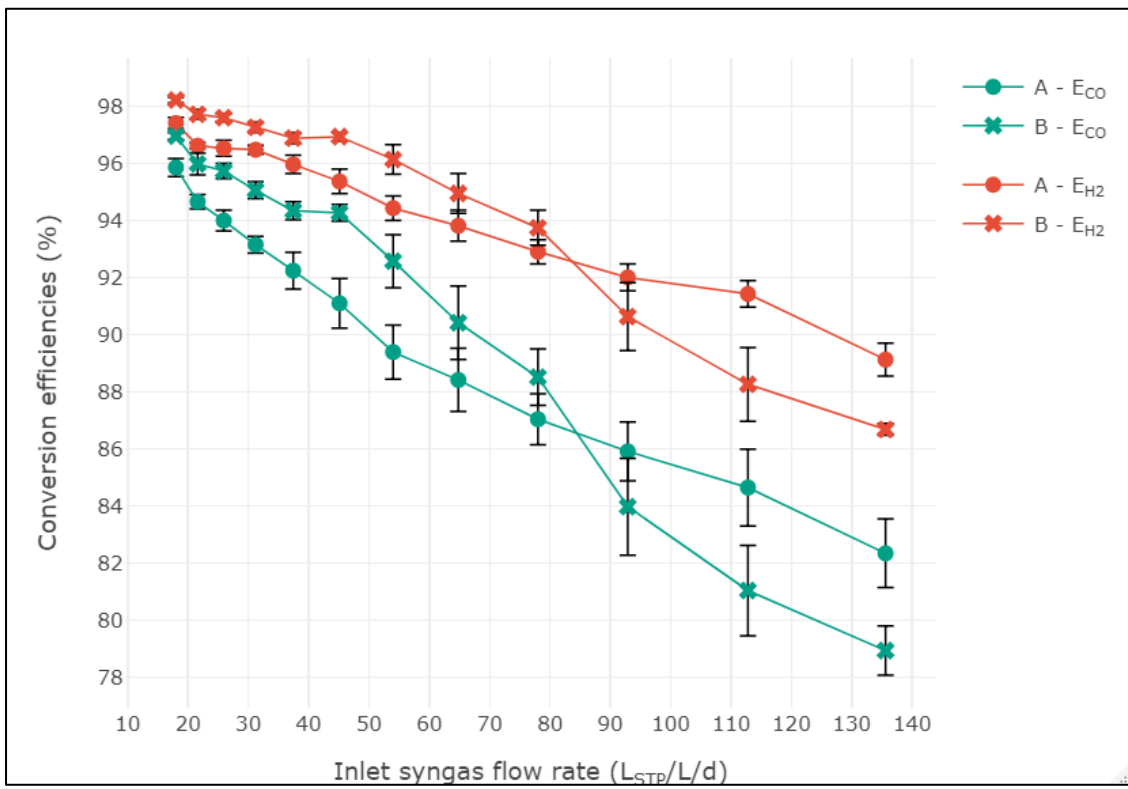


Figure 5

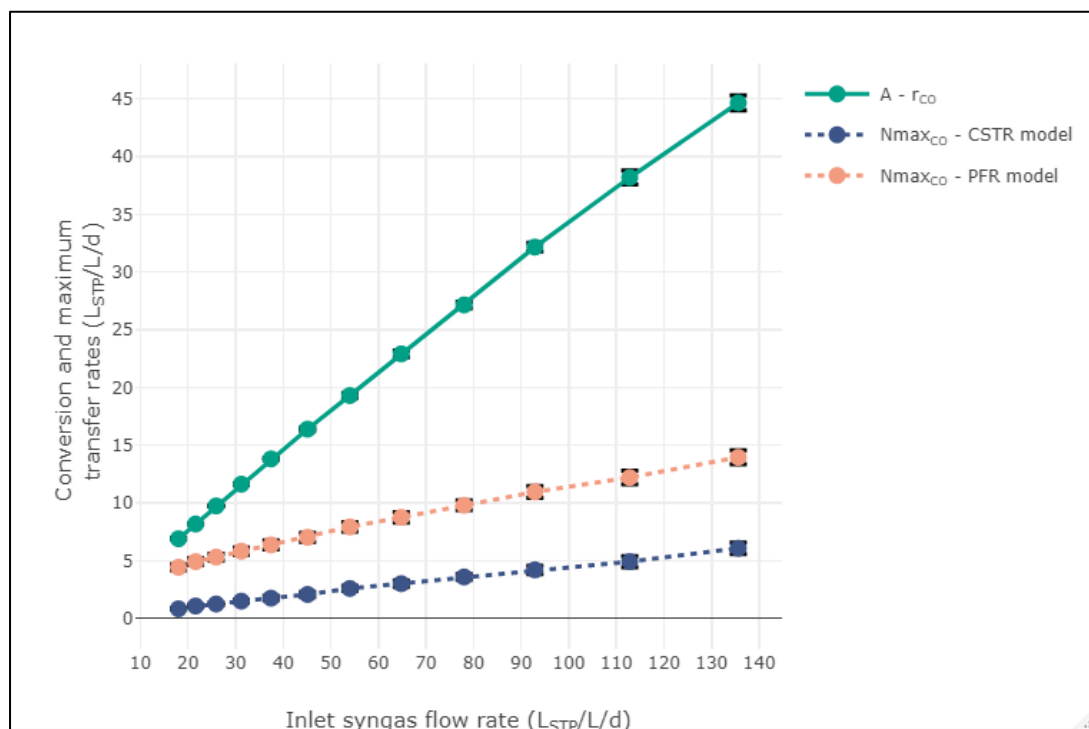


Figure 6

